IEEE Access
Multidisciplinary | Rapid Review | Open Access Journal

Received May 20, 2022, accepted June 8, 2022, date of publication June 13, 2022, date of current version June 17, 2022.

Digital Object Identifier 10.1109/ACCESS.2022.3182716

Seizure Onset Zone Identification From iEEG: A Review

SAI SANJAY BALAJI, (Graduate Student Member, IEEE) AND KESHAB K. PARHI, (Fellow, IEEE)
Department of Electrical and Computer Engineering, University of Minnesota, Minneapolis, MN 55455, USA
Corresponding author: Keshab K. Parhi (parhi@umn.edu)

ABSTRACT This paper discusses the various methods of identifying the seizure onset zone (SOZ) from the intracranial electroencephalography (iEEG) data. Epilepsy, also known as seizure disorder, is a neurological condition caused due to disruption in the regular electrical communication within the neuron network. With almost a third of epileptic conditions being drug-resistant and several cases with no known cause, there is a need to resort to alternative treatment methods such as neurostimulation or surgical resection. Both these methods require the identification of regions within the brain that need to be stimulated or resected. For most of the patients, this corresponds to the part that initiates the seizure. These are called seizure onset zone (SOZ) or epileptogenic zone (EZ). Epileptologists locate the SOZ by analyzing the iEEG data of patients suffering from seizures. This, however, is time-consuming and can be prone to human error. Thus, there has been significant research on the automatic detection of SOZ. High-frequency oscillations (HFOs), characterized by iEEG oscillations above 80 Hz, are one of the most promising candidates for identifying SOZ. Functional connectivity and graph theory measures have also distinguished SOZ and non-SOZ regions using different features. Newer works on phase-amplitude coupling have also shown promising results. With the increased data availability, it has also become possible to build supervised learning algorithms to improve the predictive power of anomaly detection algorithms used to localize SOZ.

INDEX TERMS Epilepsy, epileptogenic zone, high frequency oscillations, iEEG, seizure, seizure onset zone.

I. INTRODUCTION

Epilepsy is a neurological condition that affects the central nervous system. It is characterized by recurrent unprovoked seizures whose cause is primarily unknown [1]. With symptoms ranging from temporary loss of consciousness to increased risk of psychological conditions and premature death, epilepsy affects over 65 million worldwide [1]. Although drug delivery is a standard treatment method, at least one-third of them suffer from drug-resistant epilepsy [1]. In such cases, neurostimulation and surgical resection are two commonly suggested remedial measures. It is essential to identify the region within the brain responsible for triggering these seizures for effective treatment. These regions are called the seizure onset zones (SOZs) or epileptogenic zone.

In most cases, intracranial electroencephalography (iEEG) helps in the identification of SOZ in humans. Unlike scalp EEG, iEEG data records from electrodes surgically implanted inside patients' brains to obtain a continuous recording of the local field potentials over several hours to days [2]. The two main electrodes used are the subdural grid electrodes - an electrode array with contacts spanning across its rows and columns, and the depth electrodes - electrodes with 4 - 8 contacts placed deep inside the brain [3]. Such continuous data availability provides valuable information on the onset of seizures and the anatomical onset region. Several established works have used this data to develop practical algorithms for automated seizure detection and prediction. iEEG data can also be used to identify the onset zone from a range of biomarkers. Figure 1 illustrates the common phenomena and features that can be used as biomarker for SOZ identification. Among these biomarkers, the most researched is high-frequency oscillations [4]–[15]. Another useful measure is identifying a unique cross-frequency coupling mechanism, called phase amplitude coupling, that exists majorly in SOZs [16]–[18]. iEEG data recorded simultaneously across different cortical regions can be used

The associate editor coordinating the review of this manuscript and approving it for publication was Ludovico Minati.

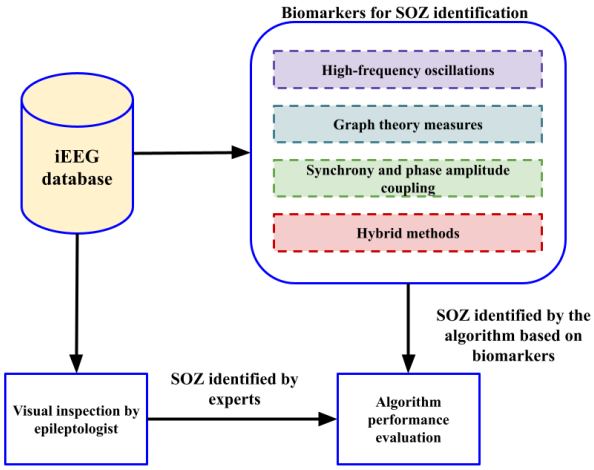

FIGURE 1. Common SOZ biomarkers - phenomena and methods.

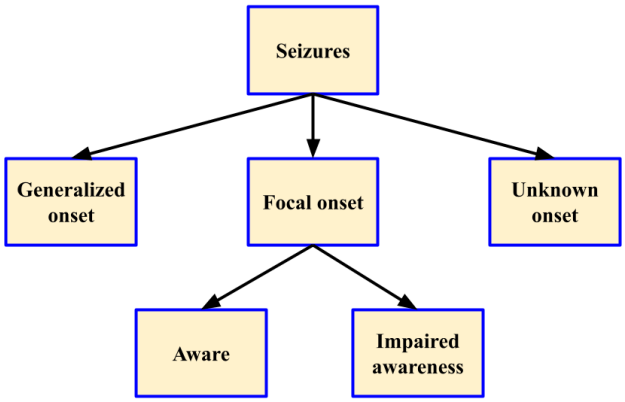

FIGURE 2. The ILAE classification of seizures [26].

to obtain directional measures of functional connectivity, represented using directed graphs. The topological features of these graphs can then be used to locate SOZ. Various methods of representing such directed graphs have been proposed in [19]–[24]. The rapid increase in the advancement of deep learning algorithms and relatively easy availability of GPUs also make it possible to develop superior deep learning models, ranging from unsupervised to supervised, to identify the SOZs using different biomarkers. This paper discusses the different established methods for identifying SOZ from iEEG data and their future implications.

The remainder of this paper is organized as follows. Section II describes the common types of seizures, characterization of the epileptic syndrome, and the concept of the epileptogenic zone or the seizure onset zone. Sections III, IV, and V, respectively, describe the recent work on identifying the SOZ from high-frequency oscillations, graph theory methods, and phase-amplitude coupling. Section VI discusses the application of Machine Learning (ML) in seizure localization. Finally, Section VII provides a comparative table of the results from important methodologies and explores the necessity to include SOZ identification algorithms in future presurgical tests.

II. EPILEPSY AND EPILEPTOGENIC ZONE

A seizure is a sudden unrestricted disruption of electrical activity across the neurons [25]. Usually caused by the local disturbances of the brain's electrical activity, seizures typically cause short-term abnormalities in muscular movements and consciousness. Although sometimes a known external reason, such as stroke or head injury, causes seizures, the cause remains unidentified in many cases. Physicians diagnose a person as epileptic when they encounter more than two unprovoked seizing episodes separated by at least one day. Epilepsy is one of the most diagnosed neurological disorders affecting around 65 million global citizens, with about 3.4 million of them in the United States [1]. Roughly half of them are diagnosed with a known cause. These can be genetic or caused by a structural change in the brain, a brain infection, or autoimmune disorder. Identification of the cause can help in curating a successful treatment strategy.

A group of features characterizes epileptic syndrome. Examples include the type of seizures, regions affected, the cause, age of onset, severity, and the frequency of attacks [1]. Seizures are broadly classified into three groups by the International League Against Epilepsy (ILAE) based on the onset, the patient's level of awareness during the seizure, and the presence/absence of motor symptoms exhibited by the patient [26]. The different groups are shown in Figure 2. Focal onset seizures, also called partial seizures, are localized, with the seizures starting in one part of the brain. Temporal lobe epilepsy (TLE) is one of the most common forms of epilepsy. It is the most common focal onset epilepsy [27]. Focal onset seizures are further classified into focal onset awareness if the person is awake and knowledgeable, and focal onset impaired awareness when the seizure affects the patient's awareness. Generalized onset seizures, also called generalized tonic-clonic or grand mal seizures, affect both the hemispheres of the brain simultaneously and frequently cause impaired cognition. When the origin of the seizure is undetected, it's categorized as an unknown onset seizure.

Localizing epilepsy has been one of the crucial tasks since its diagnosis. Some of the early work from [28] defined the concept of epileptogenic lesion responsible for epilepsy as structurally and functionally distributed tissue lesions but are operational abutting grey matter. Based on this, Jasper [29] defined the lesion area, epileptogenic focus, and the epileptogenic spikes as three concentric circles with different properties that are evident on EEG analysis. This idea has evolved over the years. From a surgical perspective, SOZ is the cortical region where seizures originate. The EZ, which refers to the crucial areas for generating seizures, is equivalent to a subsection of cortical regions that include SOZ and potential SOZ regions inferred from *irritative zone* - the cortical regions that generate interictal spikes [30].

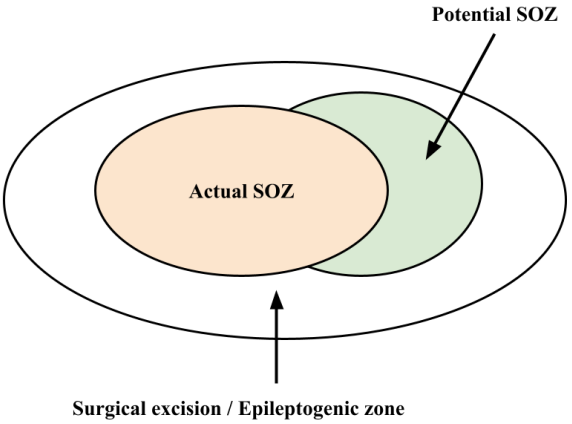

FIGURE 3. The epileptogenic zone (EZ) [31].

Resection of EZ should render patients free from seizing. Figure 3 shows the pictorial representation of the EZ encompassing the actual SOZ and potential SOZ [31]. As the location of EZ cannot be deduced directly, it is inferred mainly from SOZ. Thus, the two terms are used interchangeably [30].

Currently, SOZ localization is performed by epileptologists using visual inspection. First, magnetic resonance imaging (MRI) of the brain is used to locate focal lesions. Then, the ictal EEG or iEEG recordings of individual electrodes are inspected to identify signatures of SOZ, such as low-voltage fast activity and periodic spiking [32]. EEG recorded during sedated sleep, and sleep deprivation has shown to improve the diagnosis of epilepsy by locating sites of epileptiform discharges that were not seen in routine EEG [33]. Thus, epileptologist may also choose to record EEG (or iEEG) from patients under sedated sleep or sleep-deprived states.

III. HIGH-FREQUENCY OSCILLATIONS

A. BRAIN RHYTHMS AND FREQUENCY BANDS OF EEG

Upon inventing EEG to record the brain's electrical activities, Berger identified specific patterns of continuous recurring oscillations from the EEG recordings. He used the terms alpha and beta waves to describe these oscillatory *brain rhythms* in [34]. Since this discovery, researchers have documented numerous sustained oscillations across various mammalian brains, ranging from periods in minutes to frequencies over 600 Hz generated by different mechanisms. Furthermore, brain activity comprises multiple rhythms (frequencies) and varies over time [35]. Thus, time-frequency analysis of brain signals provide an appropriate measure of changes in frequency over time. Two standard methods for frequency decomposition are short-term Fourier transform (STFT) and wavelet transform [35]. STFT evaluates the Fourier transform within a time window that spans the time-series. A signal is decomposed by wavelet transform onto a set of basis functions called wavelets. These are obtained from scaling and time shifts of a single template, called mother wavelet [36].

TABLE 1. EEG frequency bands.

Frequency range (Hz)	Brain wave type (Bands)
1 - 4	Delta (δ)
4 - 8	Theta (θ)
8 - 13	Alpha (α)
13 - 30	Beta (β)
30 - 80	Gamma (γ)
80 - 250	Ripples
250 and above	Fast ripples

Over time, scientists grouped these oscillations into different frequency bands. Although there is no exact limit for each band, the commonly categorized bands are delta (1-4 Hz), theta (4-8 Hz), alpha (8-13 Hz), beta (13-30 Hz), gamma (30-80 Hz), ripple (80-200 Hz), and fast ripple (200-600 Hz) [37]. Based on the sampling frequency, the ripple band can be band-limited to 80-250 Hz and the fast ripple to 250-500 Hz. These frequency bands are shown in Table 1. iEEG oscillations above frequencies of 20 Hz are typically grouped as fast oscillations (FOs). FOs include beta-2 sub-band in 20 - 30 Hz, the gamma band, ripples, and fast ripples. High-frequency oscillations (HFOs), a sub-group of FOs, are characterized by at least four oscillations in the ripple or fast ripple frequency bands (80 Hz and above). HFOs occur for a relatively short duration (10–100 ms) and have a higher amplitude (10–1000 μV) than background EEG/seizures [38].

B. SOZ IDENTIFICATION FROM HFO FEATURES

The rate of HFO occurrence has been one of the predominantly used methods for analyzing the viability of HFOs as a biomarker for SOZ. The iEEG data of ten patients with intractable epilepsy was analyzed in [7]. The HFO rate (i.e., the occurrence of HFOs per minute for each electrode) was measured and it was found for all ten patients that the HFO rate, especially the rate of fast ripple, is significantly higher in SOZ channels (24.3 ± 32.4) than the non-SOZ channels (1.9 ± 4.7). It also established that HFOs occur independently of epileptic spikes, and HFO rate as a feature performed better than spikes with a high specificity of 95%. The study in [6] has shown that HFOs occur more frequently in SOZ regions than outside SOZ. The study chose ten patients undergoing presurgical evaluation from Montreal Neurological Institute with medically refractory focal seizures. HFOs were detected in seizure sections using visual inspection and the frequency spectrum was analyzed using fast Fourier transform. Results from [12], [13], and [39] that analyzed HFO rates also agreed with the above experiments. Various works have shown other features such as HFO amplitude, duration, and peak frequency can complement the HFO rate as an excellent predictive measure for seizure onset [10], [11], and [40].

Although the above results show the predominant presence of HFOs in SOZ regions, HFOs also exist in non-SOZ areas. Hence it is additionally beneficial to distinguish the two occurrences. The study of fast ripples in [11] among the 35 patients with neocortical epilepsy classified the ripples into type I and type II based on their influence in or independence from epileptiform discharges. This was characterized by the presence or absence of interictal epileptiform discharge (IED) along with the ripple event. With very high statistical significance, Type I ripple exhibited higher frequency ($p = 0.019$), less duration ($p = 0.000$), and greater amplitude($p = 0.000$) than type II ripple.

Various patient studies have identified a sharp increase in the power of fast-ripple HFOs primarily in SOZ sites during seizure onset and preceding it by several minutes. The spectral power of EEG showed a significant increase during the onset of seizures, increasing up to two times for the 40 – 50 Hz range and up to five times for the 80 – 120 Hz range [41]. Analysis of subdural EEG recorded from children with intractable seizures showed the presence of very fast oscillations few seconds before seizure onset [42]. The study in [5] found HFOs localized during the onset of seizures for all the patients analyzed. In addition to this, the high-frequency activity increased 20 minutes before the onset for most seizures. Results from [8] also showed localization of high-frequency oscillations above 100 Hz at the onset electrodes. It also showed a significant increase in the signal power of HFOs 8 seconds before the onset.

Multiple studies on epileptic surgeries have also shown that resecting brain regions having high interictal HFO events and positive surgical outcomes have a high correlation [43]–[45]. These results make HFOs a promising biomarker for SOZ identification. However, the average HFO rate, as observed from the works mentioned above, varies significantly across different brain regions. The rate is affected by sleeping patterns, indicating that it could depend on the time of the day when it's measured. The statistical analysis of iEEG recordings during non-REM sleep in [46] showed that the HFO rate, by itself, is statistically no better than spikes in localizing SOZ and is not sensitive enough to be a unique biomarker for seizure localization. It has also been demonstrated that the high correlation between the removal of HFO-generating regions and seizure-free outcomes at the group level diminished for individual analysis, and some patients became seizure-free without resecting the majority of HFO-generating regions [47]. Further work is required to understand and overcome these limitations that challenge the suitability of HFOs as a biomarker for SOZ identification.

C. HFO DETECTION USING UNSUPERVISED LEARNING

Automated detection of HFOs use some form of anomaly detector to observe the high-frequency activities and find out the aberrant activity that corresponds to ictal signals. Figure 4 shows a generalized block diagram of such an unsupervised detection system. A moving average RMS amplitude detector for the 100 – 500 Hz range is used in [4]. Using a sliding

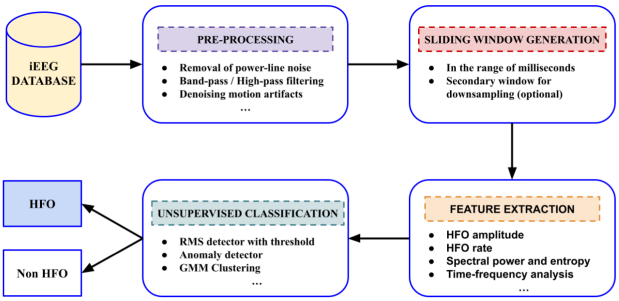

FIGURE 4. Automatic detection of high-frequency oscillations.

window of 3 ms, window sections that exceeded a threshold of 5 standard deviations from mean RMS for at least two windows were selected as HFO candidates. There was an additional threshold to identify at least six rectified peaks to label a candidate as a HFO event. In [48], the detection of HFO events occurred in stages. It used the same method as in [4] to select the HFO candidates. Then the retention of a candidate and subsequent unsupervised classification were carried out using features extracted from the power spectral density. The anomaly detection algorithm used in [14], which studied both amplitude and rates of HFOs, utilized dynamic time warping to calculate the distance of every pair of windows and clustering to separate the background cluster from the anomalous cluster (epileptogenic cluster).

Interictal spikes (IES) of EEG, which are observed for a very short duration (less than 250 ms), mainly in patients susceptible to seizures, is another highly sensitive spatial biomarker for the epileptogenic zone [49]. These, however, are not specific to the seizing zones [50] and hence are inferior to HFOs as a biomarker. The combination of IES with HFOs can provide more beneficial information in identifying the onset zone using their co-occurrence. In [15], an automatic HFO and IES detector was built using kernelized SVM. Using the intracranial EEG of eight patients from the study group and simulated data from SIMDAT, the classifier was trained using visually marked events on 25 ms windows with 50% overlap. The classifier, with an accuracy ranging from 95% to 100% and specificity of 96% to 100%, showed that IES as such performed poorly in classifying when compared to HFOs. However, the combination of IES with fast ripples or HFOs outperformed the prediction using HFOs alone. The classifier suffered from lower sensitivity in the presence of noise when used on the SIMDAT data.

It is common for iEEG recordings to contain high-frequency transients and artifacts caused due to muscle movements. These can be mistaken for HFOs without a proper preprocessing step [51]. Introducing semi-supervised learning or creating an algorithm tailormade to filter out these artifacts can result in more accurate identification. The anomaly detection techniques discussed earlier utilize different forms of thresholding operation to avoid such false positives. The HFO detection technique in [13] used an

intermediate time-frequency analysis for denoising, which eliminated spikes. Using features extracted from spectral information of high-frequency candidates, clustering was employed to identify HFO signals and segregate them from any additional noise.

IV. GRAPH THEORY BASED BRAIN CONNECTIVITY MEASURES

One of the primary goals of cognitive neuroscience is to identify the neural interactions within the brain corresponding to a specific cognitive task. By comparing these interactions during seizures with a healthy baseline, we can identify the abnormalities. Researchers have used this approach to obtain a brain map from iEEG data for analyzing epileptic patients.

The brain connectivity, as described in [52], can be predominantly classified into three types - structural connectivity, functional connectivity, and effective connectivity. *Structural/ anatomical connectivity* refers to the physical interconnection of axons emerging from a brain region connecting to another. Any of the widely available non-invasive magnetic resonance imaging techniques can identify the structural connectivity. *Functional connectivity* is a measure of the correlation or the statistical dependency between the brain regions inferred from a time-series signal. It is helpful in grouping regions of the brain into an interactive network corresponding to a cognitive task. The Pearson's correlation coefficient is a commonly used measure of functional connectivity. *Effective connectivity* represents the *directional* data flow between the brain regions during a cognitive task. It identifies a causal brain network corresponding to the directed interactions between the different areas in the brain during a cognitive task [53]. There are other ways to describe and classify brain connectivity measures. For example, complex network models are used in [54] to describe structural and functional connectivity employing small-world architectures, clustering, and quantifiable topological parameters, such as modularity, centrality, and hub distribution. In [55], functional connectivity is described as an observable phenomenon quantified with measures of statistical dependencies, and effective connectivity corresponds to the parameter of a model that tries to explain observed dependencies described by functional connectivity. Functional connectivity has been used to discriminate borderline personality disorder in [56].

The presence of hidden sources highly impacts the estimation of connectivity measures. For example, in the case of functional connectivity estimation using Pearson's correlation, two independent process variables can be highly correlated. However, neither could be a causal factor of the other, and a hidden process could be driving these two processes. Hidden factors also can lead to spurious connectivity estimates using Granger Causality measures if a common input node is not observed or the coupling strength varies between the nodes [57], [58]. This, however, can be eliminated by observing all the nodes and using re-normalization. Other factors that affect the accurate estimation of connectivity measures are signal-to-noise ratio and unequal observation periods [57]. Thus, care must be taken to minimize the noise and avoid sampling bias.

Identifying a causal relation in a complex system such as the human brain can be complicated. Scientists have developed multiple methods over the years for estimating effective connectivity. However, it is often debated if the effective connectivity measure is an actual representation of the causal interactions within the brain. This stems from the idea that a few hundred electrophysiological recordings from different regions may be insufficient to derive a brain's causal model consisting of billions of neurons, as the activities of the numerous unobserved neurons may likely have a more significant influence than the ones recorded [59]. Perhaps effective connectivity can be better described as a directional measure inferred from the statistical dependency of the time-series of iEEG recordings from the various channels.

Nonetheless, such effective connectivity measures have shown promising results in locating SOZ. For the context of this manuscript, any reference to "causal" networks refers to effective connectivity. This section reviews two main measures of effective connectivity that have been used in the literature to localize seizures. Subsection IV-A describes the works that make use of the family of Granger Causality measures, and the subsection IV-B describes works that use directed information as the causal measure in identifying SOZs. In both cases, the connectivity measures are represented using the edges of a directed graph with the different channels as the nodes. Different graph features, such as node degrees and centrality, are used to distinguish SOZ from non-SOZ channels.

A. GRANGER CAUSALITY AS THE CAUSAL MEASURE

1) THE FAMILY OF GRANGER CAUSALITY MEASURES

The statistical hypothesis test of Granger Causality (GC) [60] is one of the most popular measures in neuroscience to infer causality between two time-series. Considering two Auto Regressive (AR) time series X and Y, we can infer that X Granger causes Y if the predictability of Y improves when it is modeled using the past inputs of Y and X. To express mathematically as suggested in [61], let the time series be $X^N = [x_1, x_2, \ldots, x_N]$ and $Y^N = [y_1, y_2, \ldots, y_N]$. Consider the two different AR representations of Y:

$$y_i = \sum_{j=1}^{L} a_j y_{i-j} + e_i$$

$$y_i = \sum_{j=1}^{L} (b_j y_{i-j} + c_j x_{i-j}) + \tilde{e}_i$$

Let e_i represent the error in predicting Y from its past values alone and $\tilde{e}_i$ be the error in predicting Y from past values of both X and Y. It can be concluded that X Granger causes Y if the mean squared error of $\tilde{e}_i$ is much less than that of e_i.

GC index inferred from the AR model is used to estimate the causal interaction in the time domain. The

same concept can be extended to a multivariate AR model. Other causal measures in the GC family include Directed Transfer Function (DTF) [62] and Partial Directed Coherence (PDC) [63], which estimate the causal interaction in the frequency domain. This is useful for identifying interactions during a cognitive task predominantly observed in a particular frequency band.

2) SOZ IDENTIFICATION FROM GC MEASURES

The EEG study in [22] used an extension of Fourier and wavelet transform-based nonparametric methods to obtain GC spectra and observed the net causal outflow of each channel. The results from all eight patients showed that high-frequency GC relationships could be established among groups of channels 2 to 12 seconds before any visible ictal onset (100% positive prediction before the onset). The net causal outflow also exceeded three standard deviations (SD) from the mean value. The study of 25 patients in [64] using the Granger causal connectivity analysis (GCCA) toolbox [65] determined the causal inference among each possible pair of electrode-specific iEEG data using 20 minutes of interictal data. The visual analysis of the obtained graphs showed a concentration of ''causal nodes'' in and around the ictally active electrodes. The estimated probability of such a match by chance alone is minuscule (with probability less than 10^{-20}), suggesting the strong correlation between the derived interictal GC maps with actual ictal networks.

In contrast to the standard definition of focal seizures, [66] hypothesizes that focal seizures arise from a network rather than a single node. SOZ, in this case, is identified by the crucial node within this network, the removal of which stops seizures. Thus, identifying SOZ requires a graph theory approach within the seizure-inducing network to locate the crucial node based on local measures (node degree and centrality). Multiple past and recent works have reinforced this hypothesis. For example, DTF, proposed by [62], was used for windows of ictal and interictal clips in their study to identify the strongest 5% of the analyzed causal connections. Based on the values of betweenness centrality, the brain regions were segregated via k-means clustering [67] into active and inactive. The active regions were found to correlate with the location of the resected cortical regions in patients who were seizure-free following surgical intervention. Another example is the analysis of epileptic networks of 16 patients with TLE in [68]. Using time-varying PDC estimates of directed interaction, they showed that regions with high net outflow were concordant with the EZ estimated invasively by clinicians.

Though the family of GC measures is widely recognized for its effectiveness and simplicity, its major limitation is that GC assumes the process to be wide-sense stationary, builds an AR model for the time series, and, uses a linear predictor. This leads to poor results analyzing data that have non-linear solid interactions. Many interactions between the brain regions are non-linear, and thus, cannot be directly inferred using GC [69]. Newer methods of non-linear GC methods proposed in [70]–[73] helps to remediate the linear prediction of the GC model. Several methods have been proposed to overcome the stationarity assumption to provide time-varying functional and effective connectivity measures using GC measures. For example, [74] proposes an adaptive MVAR model using overlapped smaller time windows, and the process is assumed to be stationary within a time window. This modification was incorporated in [75] to improve the estimation of causal interaction using DTF. In contrast to stationary assumption within a small time window, [76], [77] proposed data-driven algorithms that modeled the dynamic changes in the brain network as a time-varying MVAR model using adaptive Kalman filters, with both the models providing superior estimates of the directed interactions that were in accordance with known physiology.

The work of [19] and [21] also used a modified variant of the directed transfer function to extend for time-varying MVAR model, called adaptive directed transfer function, to obtain a graphical connectivity pattern during seizure onset. The net outflow of information and out-degree measures were used to predict the onset region. The resection of regions identified in [19] resulted in elimination of seizures post-surgery. The highest total out-degree evaluated in [21] corresponded for all patients with the regions that were identified by epileptologists and were subsequently resected.

The above-discussed method is attractive for seizure localization as it is non-invasive. Traditional non-invasive EEGs, primarily used in seizure detection, suffer from poor spatial resolution – making them impractical for seizure localization. However, the combination of high-density EEG source imaging (ESI) with the functional connectivity analysis in [78] devised a non-invasive approach that overcame this limitation. The high-density EEG (HD-EEG) of five patients with refractory epilepsy, recorded for 24 hours sampled at 250 Hz or 1 kHz with 32 – 204 electrodes, was studied for this. The functional connectivity in this work was also estimated using the adaptive transfer function [21] and the SOZ was selected as the region with the highest out-degree. The brain source was reconstructed from ESI using the finite difference method (FDM) head model [79] and the LORETA algorithm [80]. This method successfully localized the SOZ for four of five patients for all setups that used at least 128 electrodes. Future enhancements of such a combined method may facilitate a non-invasive presurgical evaluation for SOZ identification.

B. DIRECTED INFORMATION (DI) AS THE CAUSAL MEASURE

A causal connectivity measure can also be inferred using *directed information*, an information-theoretic measure introduced by Massey [81]. To define this, let's consider N data samples of two channels/time-series X and Y with the same form of representation used to explain GC. The directed information from X to Y can be interpreted as the number

of bits of uncertainty in process Y that is causally explained away by the process X [23]. With reference to [23] and [82], DI can be mathematically defined as

$$I(X^N \rightarrow Y^N) = \sum_{n=1}^{N} I(X^N; y_n | Y^{n-1}).$$

DI method is not model specific, and we can apply DI to a wide range of electrical signals from the brain, such as EEG and ECoG.

In [23], a data-driven and model-based likelihood estimator is used to calculate the directed information between each pair of electrodes. Using this causal graph, the net outward flow of information was computed and the regions with the significant net outward flow were identified. Compared to a visual analysis by expert physicians, the results from the data-driven model were able to locate all the onset regions with false-positive observed in only two of the patients. An added advantage of this method is ranking the areas in decreased order of clinical relevance based on the net outward flow.

A combination of DI and GC can improve the localization of SOZ [24]. Using publicly available data from IEEG-Portal [83] (http://www.ieeg.org), [24] proposed an algorithm to automatize the SOZ identification. The algorithm involved two steps. The first step involved estimating pairwise causal influence using both the DI and GC methods. The second step of SOZ inference utilized a variant of the PageRank algorithm [84] followed by post-processing scoring. The results from 17 out of 19 patients showed successful deduction, i.e., more than 50% overlap of identified electrodes with actual onset electrodes or their immediate neighbors.

V. NEURONAL SYNCHRONY AND PHASE AMPLITUDE COUPLING

A. SYNCHRONY MEASURES AND SOZ IDENTIFICATION

The measure of synchronization in firing a large population of neurons within a network is termed neuronal *synchrony*. Synchrony is a critical measure that can characterize epilepsy. Traditionally, abnormally high and prolonged neural synchronization is presumed to result in epilepsy [85]. The *hypersynchronous* firing of a large population of neurons as epileptic seizures has been described in [86].

While the amplitude of EEG signals is a consequence and thus can correlate to the synchrony, the presence of other critical factors, mainly the degree of precision in synchronization of neuronal discharges, makes it infeasible to characterize the synchrony solely from the amplitude values [87]. Popular synchrony measures include linear cross correlation [88], [89], coherence - the covariance of amplitudes for different frequency bands, and phase correlation [90]. A few experiments have tried locating SOZ from measures of synchrony.

EEG analysis of six patients with intractable epilepsy in [91] studied synchrony measures to distinguish SOZ. One hour-long interictal EEG signals, acquired using grid and depth electrodes, were filtered with a passband of 4 - 30 Hz (theta, alpha, and beta bands). The normalized cross-correlation coefficients for a 5-sec window were used as the synchrony measure, and the regions with the highest synchrony measure were marked hypersynchronous. The synchrony pattern remained stable for the 1-hour duration, and the hypersynchronous area overlapped with the SOZs located by epileptologists in all but one patient. Though this shows a correlation between the two, it is unclear if the hypersynchronous activity causes seizures. Moreover, grid electrodes used for the analysis are placed on the brain surface and thus do not provide sufficient information to study seizures originating from deep inside the brain.

While studies on epileptic patients provide meaningful results on localizing seizures, it does not show how the brain and synchrony measures differ from a healthy person. The research work by [92] studied the local field potential (LFP) of four patients with focal partial epilepsy and two control non-epileptic subjects. The signal, acquired at 32,556 Hz using subdural grid electrodes, was later downsampled to 5 kHz for analysis. Synchrony measures of cross-correlation and mean phase coherence were obtained for 1s non-overlapping windows. The SOZ identified by clinical experts showed lower synchrony with other regions for epileptic patients when compared to the control. The lower synchrony levels led the researchers to speculate that the SOZs in epileptic patients are isolated functionally from the neighboring areas, which might be a substantial contributing factor for spontaneous epileptic activity. Three of the four patients were eligible for resective surgery and remained seizure-free after the surgery. Though this success seems to validate the former speculation of the functional disconnect of SOZs from other regions, further work is required to validate whether this contributes to seizure generation.

B. PHASE-AMPLITUDE COUPLING MEASURES AND SOZ IDENTIFICATION

The concept of neuronal synchrony can also be interpreted in terms of synchronizing interactions between various neuronal oscillations. The brain oscillations exist in varying frequencies, with lower frequencies responsible for interactions that occur over a longer time and over much larger regions, and the short-term local interactions are characterized by high-frequency bands [93]. These oscillations show a degree of dependence between each other. The different frequency bands can interact with each other, and the oscillations of one band can modulate the oscillatory response of another [94]. This phenomenon is called *cross-frequency coupling* (CFC). A major form of such interaction is called *phase-amplitude coupling* (PAC), in which the phase of lower frequency actions modulate the amplitude of high-frequency activities. Results from [95] and [96] have shown that CFC is characteristic of the ongoing brain activity and change based on the cognitive task. In addition to

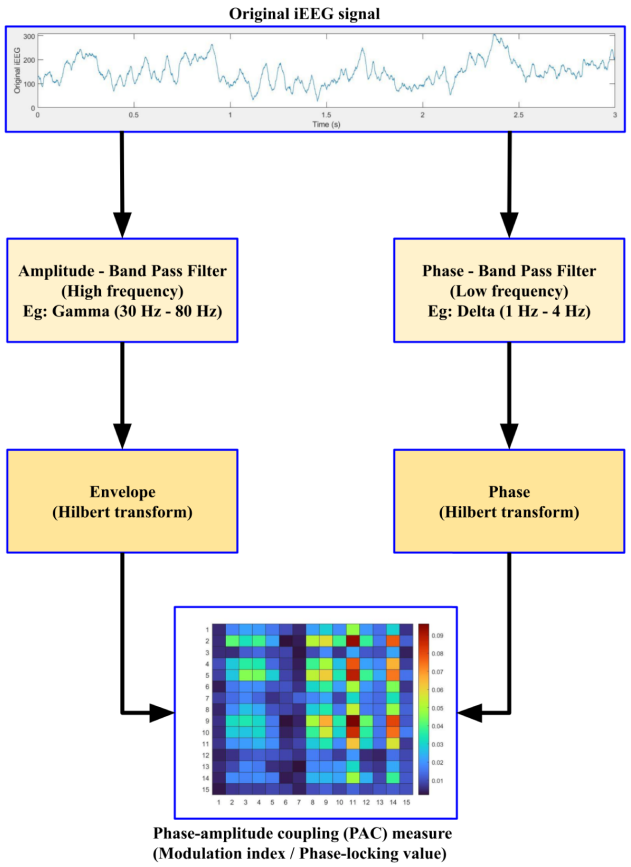

FIGURE 5. Estimation of phase-amplitude coupling.

this, the results from [97], [98], and [99] have also shown that CFC, especially that between low-frequency phase and the amplitude of high-frequency gamma of ictal iEEG data, can characterize the seizures effectively. These have led to a few recent works on characterizing the predictability of phase-amplitude coupling for the identification of SOZ [16]–[18].

With no single standard for PAC measure, there exist different techniques to quantify PAC. While each method has its pros and cons as described in [100]–[102], a popular method is the *modulation index* proposed in [103], which is based on the normalized entropy measure from [104]. Hilbert transform is used to extract the envelope of the high-frequency band and phase of the low-frequency band. The phases are binned against the mean amplitude of the HF signal for each bin. Finally, the normalized entropy measure is calculated for the modulation index (MI). Figure 5 shows the general steps in determining the measures for PAC.

This feature was used in [16] to calculate the PAC for all low- and high-frequency pairs. The first four minutes of EEG signal during each sleeping stage (N1, N2, N3, and REM) is used for analysis. The channels were grouped into either of the three classes – SOZ channels, exclusively irritative zone (EIZ, channels where spiking is observed outside SOZ), and normal zone (NoZ, channels without any epileptic incident). The PAC measure (MI) obtained for the three classes are compared, and it was seen that the MI for SOZ channels is much higher than that for the EIZ and NoZ channels for varied levels of sleep. The observations also concluded that the coupling is maximum during the deep sleep N3 stage. Prior observations from [4] and [12] that inferred the modulation of HFOs by sleep show an underlying correlation between the two phenomena. However, the study [16] did not analyze the various regions of the brain, and the role of PAC in identifying the resective area is yet to be studied. A similar analysis of the phase-locking value (PLV) of limited patients by [18] showed higher phase-amplitude coupling for electrodes near the seizure onset zone. The ripples for the range of 80 – 150 Hz and spikes of EEG data was analyzed in [17] from patients with mesial temporal lobe epilepsy while asleep. PAC is measured using two methods. The first method is by phasor transformation of the instantaneous amplitude and phase, quantifying the strength and ripple rate coupled with spikes. The second step evaluated the strength and spectral frequency of the modulating and modulated signals with a modified averaging measure. Both estimates indicated a higher coupling of ripple amplitude with the phase of epileptiform spikes inside the SOZ than outside.

Supervised machine learning in retrospective analyses has shown promising results in validating PAC as a viable biomarker for locating SOZ. For example, a logistic regression classifier was developed in [105] using PLV features of high gamma amplitude with the phase of low-frequency rhythms, extracted from ictal iEEG recordings of ten epileptic patients who underwent surgical resection. In addition to the successful location of SOZ regions for seizure-free patients post-surgery, the number of non-resected SOZ electrodes identified by the algorithm correlated with the seizure outcome in non-seizure-free patients.

Although the discussed methods indicate significantly higher PAC at SOZ regions, these are obtained from smaller studies. Their generalizability is unknown, and the actual relation between PAC with SOZ is yet to be quantified. Further work is required to confirm the viability of PAC as a biomarker for localizing seizures.

VI. MACHINE LEARNING FOR SOZ IDENTIFICATION

The increased data availability has facilitated significant utilization of machine learning (ML) algorithms for predictive tasks across numerous fields, including biological data sets. Numerous research works on brain data sets have applied machine learning for the detection and prediction of seizures with very high accuracy [106]–[110]. Seizure localization is a more complex problem as the ground truth identified by visual inspection may be subjective. One way to determine the veracity is to determine the success rate in rendering a patient seizure-free after surgical resection of the identified region.

TABLE 2. Summary of the various methods of seizure onset zone identification discussed in this paper.

Author	Year	Dataset	Electrode configuration	Sampling frequency	Analysis method	Methodology	Performance
Staba et al [4]	2002	study group (25 patients)	16 channels of depth electrodes	10 kHz	HFO	RMS detector with thresholds	accuracy = 84%
Worrell et al [5]	2004	study group (24 patients)	subdural electrodes (varying channels)	5 kHz	HFO	visual inspection, statistical analysis	HFO identified in 62% of the study group
Jirsch et al [6]	2006	study group (10 patients)	depth electrodes with average 30 channels	2 kHz	HFO	visual inspection, spectral analysis	75% accurate for mesial temporal epilepsy, unable to detect for poorly localized epilpesy
Jacobs et al [7]	2008	study group (10 patients)	depth and cortical surface electrodes	2 kHz	HFO	visual inspection of interictal HFO rate	maximum SS = 54.5% SP = 95%
Khosravani et al [8]	2009	study group (7 patients, 19 seizures)	depth and subdural grid electrodes	5 kHz	HFO	time frequency analysis, spatial distribution and temporal change of spectral bands	$p < 0.001$ for HFO localization and $p < 0.05$ for increase in HFO power
Van Mierlo et al [19]	2011	study group (1 patient, 29 seizures)	52 depth and strip electrodes	256 Hz	graph analysis	Adaptive directed transfer function	SS and SP above 95%
Wilke et al [20]	2011	study group	subdural silastic grids	500 Hz	graph analysis	betweeness centrality from directed transfer function	Wilcoxon $p < 0.05$
Matsumoto et al [10]	2013	study group (5 patients)	depth and grid electrodes	32.5 kHz	HFO	visual inspection, SVM classifier using spectral features	mean SS = 83.8%, SP = 84.6%
Wang et al [11]	2013	study group (35 patients)	stereotactic EEG or subdural grid and depth electrodes	2 kHz	Fast ripples (HFO)	time-frequency analysis and visual inspection	Type-I ripple highly specific to SOZ (statistical analysis, SP not mentioned)
Adhikari et al [22]	2013	study group (18 patients)	40-128 electrodes of depth and subdural grid type	500 Hz	Granger causality	wavelet power, GC spectra, causal outflow	100% positive prediction 2 to 12.5 sec earlier than visual inspection
Liu et al [13]	2016	study group (8 patients)	grid and depth electrodes	2 kHz	HFO	time frequency analysis and clustering using spectral features	mean SE = 80.7%, SP = 95.7% during sleep stage
Malladi et al [23]	2016	study group (5 subjects)	120-150 electrodes (depth and grid types)	1 kHz	net outward flow from causal graph	uses directed information	success rate 0.895, FPR 0.03
Amiri et al [16]	2016	study group (82 subjects)	depth and scalp electrodes	2 kHz	PAC	statistical analysis of PAC during different sleep stages	$p < 0.01$ for delta and alpha bands
Weiss et al [17]	2016	study group (12 patients)	depth electrodes	2 kHz	PAC	phasor transform and ripple-triggered averaging methods	high coupling of ripple amplitude and spike phase at SOZ, $p < 0.01$
Elahian et al [105]	2017	study group (10 patients)	12-80 subdural grid and strip electrodes	1kHz	PAC	logistic regression classifier	accuracy = 96%
Murin et al [24]	2018	iEEG Portal	grid type electrodes	500 Hz - 5 kHz	net outward flow from causal graph	Granger causality and directed information	100% identification, FP in 2 patients
Varatharajah et al [111]	2018	study group (82 subjects)	4- or 8- contact depth array	32 kHz	HFO, IED and PAC	SVM classifier; leave 1 out CV	SS=57.45%, SP=79.49%, AUC=0.73
Lai et al [112]	2019	study group	46-110 subdural grid electrodes	4096 Hz	HFO	CNN classifier	SS(ripple) = 88.16% SS(fast ripple) = 93.37%
Cámpora et al [18]	2019	study group (5 patients)	44-52 depth electrodes	2 kHz	PAC	phase locking value between different frequency bands	PLV higher during ictal stages, $p < 0.01$
Charupanit et al [14]	2020	study group (11 subjects)	depth electrodes	2-5 kHz	HFO	automatic detection of HFO rate and amplitude using clustering and RMS methods	mean SS = $85 - 94\%$, FPR = $6.1 - 13.7\%$
Lachner-Piza et al [15]	2020	study group and SIMDAT	depth, gridarrays and strip	1024 - 2500 Hz	HFO and IES	automatic detector using SVM	SS = $38\% - 96\%$, SP = 100%

As discussed in section III, unsupervised ML algorithms, such as clustering and anomaly detection, are predominantly used in the automated identification of HFOs. These algorithms have been shown to locate SOZ with high accuracy, evidenced by the successful correspondence with the resected regions that rendered patients seizure-free. Unsupervised clustering based on graph features from connectivity measures, discussed in section IV-A, has also been shown to distinguish SOZ channels from non-SOZ accurately.

Supervised ML algorithms rely on class labels of regions (SOZ and non-SOZ) provided by epileptologists. The classifier features are mainly extracted from the discussed biomarkers. Some specific examples are discussed in the previous sections. As discussed earlier, each biomarker by itself has minor shortcomings. Thus, combining features from multiple biomarkers might improve the predictive strength. This was done in [111] where a SOZ detection algorithm was developed using the local values of HFOs, interictal epileptiform discharges (IED), and PAC as features for an SVM classifier. The results showed that the combined classifier outperformed both unsupervised classification and classification using individual components with an AUC of 0.79.

The deluge of data availability has also facilitated the burgeoning of neural network-based algorithms for improved localization of SOZ. Deep neural network (DNN) models can be used to more accurately identify viable biomarkers of SOZ when compared to standard ML algorithms. For example, the convolutional neural network (CNN) model with time-frequency maps as features in [112] detects HFOs with improved specificity when compared to conventional unsupervised and supervised ML methods. The analysis of twelve patients from two independent datasets in [113] also shows the generalizability of the long short-term memory (LSTM) model for HFO identification. Newer works have also shown the success of DNN algorithms in identifying SOZ from non-invasive recordings, such as scalp EEG, that directly learn from the spatial and temporal features of the EEG recordings. For example, the SZLoc architecture, proposed in [114], utilizes different CNN encodings for local and global networks and combines the representation using a transformer layer. The algorithm shows superior predictability using scalp EEG (with a mean accuracy of 71.1%) and is generalizable across independent datasets. However, the performance accuracy is less than ML-based methods utilizing iEEG recordings. The above-discussed results indicate that DNN can be a useful presurgical tool to analyze a large amount of data in a much shorter time.

VII. CONCLUSION

Localizing seizure onset from iEEG can be posed as a classification task to separate electrodes into SOZ and non-SOZ. Various phenomena that are characteristic of the iEEG data from the onset zone are discussed in this paper. Table 2 summarizes the data, methodology, and performance of some essential methods discussed in this manuscript. One of the most extensively studied electrophysiological biomarkers is HFOs. To the most extent, the identification of HFO activities is performed using unsupervised learning methods for anomaly detection, such as clustering. Semi-supervised algorithms that have shown to outperform unsupervised methods [115], [116] can be incorporated to improve the detection. An alternate approach is the evaluation of brain networks using graph theory and information-theoretic methods to characterize the signal flow within the observed channels. Measures of synchrony and PAC have also shown increased coupling of specific frequency bands, which can be used to localize SOZ. ML has also been shown to improve SOZ identification and make it possible to analyze extensive data rapidly.

However, the true success of an algorithm in identifying SOZ lies in rendering the patient seizure-free after resecting the tissue from the identified regions. Unfortunately, most discussed methods are either retrospective or performed in conjunction with the physician's analysis. The final decision for resective surgeries is still performed by visual inspection. Although the role of physicians and epileptologists in locating SOZ is indisputable, analysis of iEEG recordings becomes more time-consuming with the increase in channel density. Furthermore, resection based on visual inspection sometimes results in unsatisfactory surgical outcomes. For example, the analysis of 414 patients in [117] concluded that visual inspection of the ictal iEEG recordings resulted in absolute seizure freedom only in 61%, 47%, and 42% of patients at one, three, and ten years post-surgery, respectively. The concordance of SOZ regions identified by automated algorithms and physicians, and the higher correlation of ML algorithm-identified regions with seizure outcomes in non-seizure-free patients, indicates that future clinical decisions might benefit from the inclusion of automated analysis of iEEG signals.

Although iEEG is the gold standard for seizure analysis, its invasive nature drives researchers to find non-invasive alternatives with similar performance. Recent efforts have focused on less invasive scalp EEGs and inference using source imaging techniques to identify SOZs from the different biomarkers [78], [118]. However, the attachment of several electrodes for a long duration still creates discomfort for the patients. This necessitates newer non-invasive techniques of similar performance. The work in [119] uses wavelet-based Maximum Entropy on the Mean method on the magnetic and electric source imaging of the SOZ from MEG and EEG recordings during the ictal stage. The proposed method showed 90% concordance of magnetic source imaging results with the clinical SOZ. Unlike seizure detection or prediction classification problems, which can now be classified with very high accuracy, identifying the seizure onset zone is not easy. Although there has been significant progress in this problem, as seen from this paper, more work is required for an automated identification algorithm to be used clinically. The continuous improvement of imaging techniques and incorporation of deep neural networks in future works may accurately localize SOZ.

REFERENCES

[1] *Epilepsy Foundation*. Accessed: Jun. 1, 2020. [Online]. Available: https://www.epilepsy.com

[2] J. P. Lachaux, D. Rudrauf, and P. Kahane, "Intracranial EEG and human brain mapping," *J. Physiol.-Paris*, vol. 97, nos. 4–6, pp. 613–628, Jul. 2003.

[3] A. Shah and S. Mittal, "Invasive electroencephalography monitoring: Indications and presurgical planning," *Ann. Indian Acad. Neurol.*, vol. 17, no. 5, p. 89, 2014.

[4] R. J. Staba, C. L. Wilson, A. Bragin, I. Fried, and J. Engel, Jr., "Quantitative analysis of high-frequency oscillations (80–500 Hz) recorded in human epileptic hippocampus and entorhinal cortex," *J. Neurophysiol.*, vol. 88, pp. 1743–1752, Oct. 2002.

[5] G. A. Worrell, L. Parish, S. D. Cranstoun, R. Jonas, G. Baltuch, and B. Litt, "High-frequency oscillations and seizure generation in neocortical epilepsy," *Brain*, vol. 127, no. 7, pp. 1496–1506, Jul. 2004.

[6] J. D. Jirsch, E. Urrestarazu, P. LeVan, A. Olivier, F. Dubeau, and J. Gotman, "High-frequency oscillations during human focal seizures," *Brain*, vol. 129, pp. 1593–1608, Jun. 2006.

[7] J. Jacobs, P. LeVan, R. Chander, J. Hall, F. Dubeau, and J. Gotman, "Interictal high-frequency oscillations (80–500 Hz) are an indicator of seizure onset areas independent of spikes in the human epileptic brain," *Epilepsia*, vol. 49, pp. 1893–1907, Nov. 2008.

[8] H. Khosravani, N. Mehrotra, M. Rigby, W. J. Hader, C. R. Pinnegar, N. Pillay, S. Wiebe, and P. Federico, "Spatial localization and time-dependant changes of electrographic high frequency oscillations in human temporal lobe epilepsy," *Epilepsia*, vol. 50, no. 4, pp. 605–616, Apr. 2009.

[9] N. von Ellenrieder, L. P. Andrade-Valença, F. Dubeau, and J. Gotman, "Automatic detection of fast oscillations (40–200Hz) in scalp EEG recordings," *Clin. Neurophysiol.*, vol. 123, no. 4, pp. 670–680, Apr. 2012.

[10] A. Matsumoto, B. H. Brinkmann, S. M. Stead, J. Matsumoto, M. T. Kucewicz, W. R. Marsh, F. Meyer, and G. Worrell, "Pathological and physiological high-frequency oscillations in focal human epilepsy," *J. Neurophysiol.*, vol. 110, no. 8, pp. 1958–1964, 2013.

[11] S. Wang, I. Z. Wang, J. C. Bulacio, J. C. Mosher, J. Gonzalez-Martinez, A. V. Alexopoulos, I. M. Najm, and N. K. So, "Ripple classification helps to localize the seizure-onset zone in neocortical epilepsy," *Epilepsia*, vol. 54, no. 2, pp. 370–376, Feb. 2013.

[12] M. Dümpelmann, J. Jacobs, and A. Schulze-Bonhage, "Temporal and spatial characteristics of high frequency oscillations as a new biomarker in epilepsy," *Epilepsia*, vol. 56, no. 2, pp. 197–206, Feb. 2015.

[13] S. Liu, Z. Sha, A. Sencer, A. Aydoseli, N. Bebek, A. Abosch, T. Henry, C. Gurses, and N. F. Ince, "Exploring the time–frequency content of high frequency oscillations for automated identification of seizure onset zone in epilepsy," *J. Neural Eng.*, vol. 13, no. 2, Apr. 2016, Art. no. 026026.

[14] K. Charupanit, I. Sen-Gupta, J. J. Lin, and B. A. Lopour, "Amplitude of high frequency oscillations as a biomarker of the seizure onset zone," *Clin. Neurophysiol.*, vol. 131, no. 11, pp. 2542–2550, Nov. 2020.

[15] D. Lachner-Piza, J. Jacobs, J. C. Bruder, A. Schulze-Bonhage, T. Stieglitz, and M. Dümpelmann, "Automatic detection of high-frequency-oscillations and their sub-groups co-occurring with interictal-epileptic-spikes," *J. Neural Eng.*, vol. 17, no. 1, Jan. 2020, Art. no. 016030.

[16] M. Amiri, B. Frauscher, and J. Gotman, "Phase-amplitude coupling is elevated in deep sleep and in the onset zone of focal epileptic seizures," *Front. Hum. Neurosci.*, vol. 10, p. 387, Aug. 2016.

[17] S. A. Weiss, I. Orosz, N. Salamon, S. Moy, L. Wei, M. A. Van't Klooster, R. T. Knight, R. M. Harper, A. Bragin, I. Fried, J. Engel, and R. J. Staba, "Ripples on spikes show increased phase-amplitude coupling in mesial temporal lobe epilepsy seizure-onset zones," *Epilepsia*, vol. 57, no. 11, pp. 1916–1930, Nov. 2016.

[18] N. E. Cámpora, C. J. Mininni, S. Kochen, and S. E. Lew, "Seizure localization using pre ictal phase-amplitude coupling in intracranial electroencephalography," *Sci. Rep.*, vol. 9, no. 1, pp. 1–8, Dec. 2019.

[19] P. van Mierlo, E. Carrette, H. Hallez, K. Vonck, D. Van Roost, P. Boon, and S. Staelens, "Accurate epileptogenic focus localization through time-variant functional connectivity analysis of intracranial electroencephalographic signals," *NeuroImage*, vol. 56, no. 3, pp. 1122–1133, Jun. 2011.

[20] C. Wilke, G. Worrell, and B. He, "Graph analysis of epileptogenic networks in human partial epilepsy," *Epilepsia*, vol. 52, no. 1, pp. 84–93, Jan. 2011.

[21] P. van Mierlo, E. Carrette, H. Hallez, R. Raedt, A. Meurs, S. Vandenberghe, D. Van Roost, P. Boon, S. Staelens, and K. Vonck, "Ictal-onset localization through connectivity analysis of intracranial EEG signals in patients with refractory epilepsy," *Epilepsia*, vol. 54, no. 8, pp. 1409–1418, Aug. 2013.

[22] B. M. Adhikari, C. M. Epstein, and M. Dhamala, "Localizing epileptic seizure onsets with Granger causality," *Phys. Rev. E, Stat. Phys. Plasmas Fluids Relat. Interdiscip. Top.*, vol. 88, no. 3, Sep. 2013, Art. no. 030701.

[23] R. Malladi, G. Kalamangalam, N. Tandon, and B. Aazhang, "Identifying seizure onset zone from the causal connectivity inferred using directed information," *IEEE J. Sel. Topics Signal Process.*, vol. 10, no. 7, pp. 1267–1283, Oct. 2016.

[24] Y. Murin, J. Kim, J. Parvizi, and A. Goldsmith, "SozRank: A new approach for localizing the epileptic seizure onset zone," *PLoS Comput. Biol.*, vol. 14, no. 1, 2018, Art. no. e1005953.

[25] *Types of Seizures*. Accessed: Jun. 1, 2021. [Online]. Available: https://www.hopkinsmedicine.org/health/conditions-and-diseases/epilepsy/types-of-seizures

[26] I. E. Scheffer, "ILAE classification of the epilepsies: Position paper of the ILAE commission for classification and terminology," *Epilepsia*, vol. 58, no. 4, pp. 512–521, Apr. 2017.

[27] *Temporal Lobe Epilepsy (TLE)*. Accessed: Jun. 1, 2021. [Online]. Available: https://www.epilepsy.com/learn/types-epilepsy-syndromes/temporal-lobe-epilepsy-aka-tle

[28] W. Penfield, "Epileptogenic lesions," *Acta Neurol. Belg.*, vol. 56, pp. 75–88, Jan. 1956.

[29] H. H. Jasper, G. Arfel-Capdeville, and T. Rasmussen, "Evaluation of EEG and cortical electrographic studies for prognosis of seizures following surgical excision of epileptogenic lesions," *Epilepsia*, vol. 2, no. 2, pp. 130–137, 1961.

[30] F. Rosenow and H. Lüders, "Presurgical evaluation of epilepsy," *Brain*, vol. 124, no. 9, pp. 1683–1700, Sep. 2001.

[31] H. O. Lüders, I. Najm, D. Nair, P. Widdess-Walsh, and W. Bingman, "The epileptogenic zone: General principles," *Epileptic Disorders*, vol. 8, no. 2, pp. 1–9, 2006.

[32] E. Niedermeyer and F. L. da Silva, *Electroencephalography: Basic Principles, Clinical Applications, and Related Fields*. Philadelphia, PA, USA: Lippincott Williams & Wilkins, 2005.

[33] A. J. Rowan, R. J. Veldhuisen, and N. J. D. Nagelkerke, "Comparative evaluation of sleep deprivation and sedated sleep EEGs as diagnostic aids in epilepsy," *Electroencephalogr. Clin. Neurophysiol.*, vol. 54, no. 4, pp. 357–364, Oct. 1982.

[34] H. I. Berger, "Über das elektrenkephalogramm des menschen," *Eur. Arch. Psychiatry Clin. Neurosci.*, vol. 87, pp. 527–570, Dec. 1928.

[35] G. Buzsaki, *Rhythms of the Brain*. London, U.K.: Oxford Univ. Press, 2006.

[36] N. Hazarika, J. Z. Chen, A. C. Tsoi, and A. Sergejew, "Classification of EEG signals using the wavelet transform," *Signal Process.*, vol. 59, pp. 61–72, May 1997.

[37] R. J. Staba, M. Stead, and G. A. Worrell, "Electrophysiological biomarkers of epilepsy," *Neurotherapeutics*, vol. 11, no. 2, pp. 334–346, Apr. 2014.

[38] A. Bragin, J. Engel, C. L. Wilson, I. Fried, and G. W. Mathern, "Hippocampal and entorhinal cortex high-frequency oscillations (100–500 Hz) in human epileptic brain and in kainic acid-treated rats with chronic seizures," *Epilepsia*, vol. 40, no. 2, pp. 127–137, Feb. 1999.

[39] U. Malinowska, G. K. Bergey, J. Harezlak, and C. C. Jouny, "Identification of seizure onset zone and preictal state based on characteristics of high frequency oscillations," *Clin. Neurophysiol.*, vol. 126, no. 8, pp. 1505–1513, Aug. 2015.

[40] R. Alkawadri, N. Gaspard, I. I. Goncharova, D. D. Spencer, J. L. Gerrard, H. Zaveri, R. B. Duckrow, H. Blumenfeld, and L. J. Hirsch, "The spatial and signal characteristics of physiologic high frequency oscillations," *Epilepsia*, vol. 55, no. 12, pp. 1986–1995, Dec. 2014.

[41] S. Arroyo and S. Uematsu, "High-frequency EEG activity at the start of seizures," *J. Clin. Neurophysiol.*, vol. 9, no. 3, pp. 441–448, Jul. 1992.

[42] R. D. Traub, M. A. Whittington, E. H. Buhl, F. E. N. LeBeau, A. Bibbig, S. Boyd, H. Cross, and T. Baldeweg, "A possible role for gap junctions in generation of very fast EEG oscillations preceding the onset of, and perhaps initiating, seizures," *Epilepsia*, vol. 42, pp. 153–170, May 2003.

[43] H. Fujiwara, H. M. Greiner, K. H. Lee, K. D. Holland-Bouley, J. H. Seo, T. Arthur, F. T. Mangano, J. L. Leach, and D. F. Rose, "Resection of ictal high-frequency oscillations leads to favorable surgical outcome in pediatric epilepsy," *Epilepsia*, vol. 53, no. 9, pp. 1607–1617, 2012.

[44] C. Haegelen, P. Perucca, C.-E. Châtillon, L. Andrade-Valença, R. Zelmann, J. Jacobs, D. L. Collins, F. Dubeau, A. Olivier, and J. Gotman, "High-frequency oscillations, extent of surgical resection, and surgical outcome in drug-resistant focal epilepsy," *Epilepsia*, vol. 54, no. 5, pp. 848–857, 2013.
[45] J. R. Cho, D. L. Koo, E. Y. Joo, D. W. Seo, S.-C. Hong, P. Jiruska, and S. B. Hong, "Resection of individually identified high-rate high-frequency oscillations region is associated with favorable outcome in neocortical epilepsy," *Epilepsia*, vol. 55, no. 11, pp. 1872–1883, Nov. 2014.
[46] N. Roehri, F. Pizzo, S. Lagarde, I. Lambert, A. Nica, A. McGonigal, B. Giusiano, F. Bartolomei, and C.-G. Bénar, "High-frequency oscillations are not better biomarkers of epileptogenic tissues than spikes," *Ann. Neurol.*, vol. 83, no. 1, pp. 84–97, Jan. 2018.
[47] J. Jacobs, J. Y. Wu, P. Perucca, R. Zelmann, M. Mader, F. Dubeau, G. W. Mathern, A. Schulze-Bonhage, and J. Gotman, "Removing high-frequency oscillations: A prospective multicenter study on seizure outcome," *Neurology*, vol. 91, no. 11, pp. e1040–e1052, Sep. 2018.
[48] J. A. Blanco, M. Stead, A. Krieger, J. Viventi, W. R. Marsh, K. H. Lee, G. A. Worrell, and B. Litt, "Unsupervised classification of high-frequency oscillations in human neocortical epilepsy and control patients," *J. Neurophysiol.*, vol. 104, no. 5, pp. 2900–2912, Nov. 2010.
[49] K. J. Staley and F. E. Dudek, "Interictal spikes and epileptogenesis," *Epilepsy Currents*, vol. 6, no. 6, pp. 199–202, Nov. 2006.
[50] A. A. Ward, "The epileptic spike," *Epilepsia*, vol. 1, nos. 1–5, pp. 600–606, Jan. 1959.
[51] C. G. Bénar, L. Chauvière, F. Bartolomei, and F. Wendling, "Pitfalls of high-pass filtering for detecting epileptic oscillations: A technical note on 'false' ripples," *Clin. Neurophysiol.*, vol. 121, no. 3, pp. 301–310, Mar. 2010.
[52] A. Roebroeck, A. K. Seth, and P. Valdes-Sosa, "Causal time series analysis of functional magnetic resonance imaging data," in *Proc. NIPS Mini-Symp. Causality Time Ser.*, 2011, pp. 65–94.
[53] S. Avvaru, N. Peled, N. R. Provenza, A. S. Widge, and K. K. Parhi, "Region-level functional and effective network analysis of human brain during cognitive task engagement," *IEEE Trans. Neural Syst. Rehabil. Eng.*, vol. 29, pp. 1651–1660, 2021.
[54] E. Bullmore and O. Sporns, "Complex brain networks: Graph theoretical analysis of structural and functional systems," *Nature Rev. Neurosci.*, vol. 10, no. 3, pp. 186–198, Mar. 2009.
[55] K. J. Friston, "Functional and effective connectivity: A review," *Brain Connectivity*, vol. 1, no. 1, pp. 13–36, 2011.
[56] T. Xu, K. R. Cullen, B. Mueller, M. W. Schreiner, K. O. Lim, S. C. Schulz, and K. K. Parhi, "Network analysis of functional brain connectivity in borderline personality disorder using resting-state fMRI," *NeuroImage, Clin.*, vol. 11, pp. 302–315, Jan. 2016.
[57] A. M. Bastos and J.-M. Schoffelen, "A tutorial review of functional connectivity analysis methods and their interpretational pitfalls," *Frontiers Syst. Neurosci.*, vol. 9, p. 175, Jan. 2016.
[58] P. A. Stokes and P. L. Purdon, "A study of problems encountered in Granger causality analysis from a neuroscience perspective," *Proc. Nat. Acad. Sci. USA*, vol. 114, no. 34, Aug. 2017, Art. no. E7063.
[59] D. M. A. Mehler and K. P. Kording, "The lure of misleading causal statements in functional connectivity research," 2018, *arXiv:1812.03363*.
[60] C. W. Granger, "Investigating causal relations by econometric models and cross-spectral methods," *Econometrica, J. Econ. Soc.*, vol. 37, no. 3, pp. 424–438, Aug. 1969.
[61] Z. Wang, A. Alahmadi, D. C. Zhu, and T. Li, "Causality analysis of fMRI data based on the directed information theory framework," *IEEE Trans. Biomed. Eng.*, vol. 63, no. 5, pp. 1002–1015, May 2016.
[62] M. J. Kaminski and K. J. Blinowska, "A new method of the description of the information flow in the brain structures," *Biol. Cybern.*, vol. 65, no. 3, pp. 203–210, 1991.
[63] L. A. Baccalá and K. Sameshima, "Partial directed coherence: A new concept in neural structure determination," *Biol. Cybern.*, vol. 84, no. 6, pp. 463–474, May 2001.
[64] E.-H. Park and J. R. Madsen, "Granger causality analysis of interictal iEEG predicts seizure focus and ultimate resection," *Neurosurgery*, vol. 82, no. 1, pp. 99–109, 2018.
[65] A. K. Seth, "A MATLAB toolbox for Granger causal connectivity analysis," *J. Neurosci. Methods*, vol. 186, pp. 262–273, Sep. 2010.
[66] M. P. Richardson, "Large scale brain models of epilepsy: Dynamics meets connectomics," *J. Neurol., Neurosurg. Psychiatry*, vol. 83, no. 12, pp. 1238–1248, Dec. 2012.
[67] A. Likas, N. Vlassis, and J. J. Verbeek, "The global k-means clustering algorithm," *Pattern Recognit.*, vol. 36, no. 2, pp. 451–461, Feb. 2003.
[68] A. Coito, G. Plomp, M. Genetti, E. Abela, R. Wiest, M. Seeck, C. M. Michel, and S. Vulliemoz, "Dynamic directed interictal connectivity in left and right temporal lobe epilepsy," *Epilepsia*, vol. 56, no. 2, pp. 207–217, Feb. 2015.
[69] O. David, I. Guillemain, S. Saillet, S. Reyt, C. Deransart, C. Segebarth, and A. Depaulis, "Identifying neural drivers with functional MRI: An electrophysiological validation," *PLoS Biol.*, vol. 6, no. 12, p. e315, Dec. 2008.
[70] B. P. Bezruchko, V. I. Ponomarenko, M. D. Prokhorov, D. A. Smirnov, and P. A. Tass, "Modeling nonlinear oscillatory systems and diagnostics of coupling between them using chaotic time series analysis: Applications in neurophysiology," *Physics-Uspekhi*, vol. 51, no. 3, pp. 304–310, 2008.
[71] D. Marinazzo, M. Pellicoro, and S. Stramaglia, "Kernel method for nonlinear Granger causality," *Phys. Rev. Lett.*, vol. 100, no. 14, 2008, Art. no. 144103.
[72] M. Hu and H. Liang, "A copula approach to assessing Granger causality," *NeuroImage*, vol. 100, pp. 125–134, Oct. 2014.
[73] D. Marinazzo, W. Liao, H. Chen, and S. Stramaglia, "Nonlinear connectivity by Granger causality," *NeuroImage*, vol. 58, no. 2, pp. 330–338, Sep. 2011.
[74] M. Ding, S. L. Bressler, W. Yang, and H. Liang, "Short-window spectral analysis of cortical event-related potentials by adaptive multivariate autoregressive modeling: Data preprocessing, model validation, and variability assessment," *Biological*, vol. 83, pp. 35–45, Jun. 2000.
[75] M. Kamiński, M. Ding, W. A. Truccolo, and S. L. Bressler, "Evaluating causal relations in neural systems: Granger causality, directed transfer function and statistical assessment of significance," *Biol. Cybern.*, vol. 85, no. 2, pp. 145–157, Aug. 2001.
[76] M. F. Pagnotta and G. Plomp, "Time-varying MVAR algorithms for directed connectivity analysis: Critical comparison in simulations and benchmark EEG data," *PLoS ONE*, vol. 13, no. 6, Jun. 2018, Art. no. e0198846.
[77] D. Pascucci, M. Rubega, and G. Plomp, "Modeling time-varying brain networks with a self-tuning optimized Kalman filter," *PLOS Comput. Biol.*, vol. 16, no. 8, Aug. 2020, Art. no. e1007566.
[78] W. Staljanssens, G. Strobbe, R. V. Holen, G. Birot, M. Gschwind, M. Seeck, S. Vandenberghe, S. Vulliémoz, and P. van Mierlo, "Seizure onset zone localization from ictal high-density EEG in refractory focal epilepsy," *Brain Topography*, vol. 30, no. 2, pp. 257–271, Mar. 2017.
[79] H. Hallez, B. Vanrumste, P. Van Hese, Y. D'Asseler, I. Lemahieu, and R. Van de Walle, "A finite difference method with reciprocity used to incorporate anisotropy in electroencephalogram dipole source localization," *Phys. Med. Biol.*, vol. 50, no. 16, p. 3787, 2005.
[80] R. D. Pascual-Marqui, C. M. Michel, and D. Lehmann, "Low resolution electromagnetic tomography: A new method for localizing electrical activity in the brain," *Int. J. Psychophysiol.*, vol. 18, no. 1, pp. 49–65, Oct. 1994.
[81] J. Massey, "Causality, feedback and directed information," in *Proc. Int. Symp. Inf. Theory Applic. (ISITA)*. Princeton, NJ, USA: Citeseer, 1990, pp. 303–305.
[82] Y. Liu and S. Aviyente, "Directed information measure for quantifying the information flow in the brain," in *Proc. Annu. Int. Conf. IEEE Eng. Med. Biol. Soc.*, Sep. 2009, pp. 2188–2191.
[83] J. B. Wagenaar, B. H. Brinkmann, Z. Ives, G. A. Worrell, and B. Litt, "A multimodal platform for cloud-based collaborative research," in *Proc. 6th Int. IEEE/EMBS Conf. neural Eng. (NER)*, Nov. 2013, pp. 1386–1389.
[84] L. Page, S. Brin, R. Motwani, and T. Winograd, "The PageRank citation ranking: Bringing order to the web," Stanford InfoLab, Stanford, CA, USA, Tech. Rep. 1999-66, 1999.
[85] W. Penfield and H. Jasper, "Epilepsy and the functional anatomy of the human brain," *JAMA*, vol. 155, no. 1, p. 86, 1954, doi: 10.1001/jama.1954.03690190092039.
[86] R. S. Fisher, "Epileptic seizures and epilepsy: Definitions proposed by the international league against epilepsy (ILAE) and the international bureau for epilepsy (IBE)," *Epilepsia*, vol. 46, no. 4, pp. 470–472, 2005.
[87] P. J. Uhlhaas and W. Singer, "Neural synchrony in brain disorders: Relevance for cognitive dysfunctions and pathophysiology," *Neuron*, vol. 52, no. 1, pp. 155–168, Oct. 2006.
[88] A. Aarabi, F. Wallois, and R. Grebe, "Does spatiotemporal synchronization of EEG change prior to absence seizures?" *Brain Res.*, vol. 1188, pp. 207–221, Jan. 2008.

[89] M. A. Kramer, E. D. Kolaczyk, and H. E. Kirsch, "Emergent network topology at seizure onset in humans," *Epilepsy Res.*, vol. 79, pp. 173–186, May 2008.
[90] F. Mormann, K. Lehnertz, P. David, and C. E. Elger, "Mean phase coherence as a measure for phase synchronization and its application to the EEG of epilepsy patients," *Phys. D, Nonlinear Phenomena*, vol. 144, nos. 3–4, pp. 358–369, 2000.
[91] J. Dauwels, E. Eskandar, and S. Cash, "Localization of seizure onset area from intracranial non-seizure EEG by exploiting locally enhanced synchrony," in *Proc. Annu. Int. Conf. IEEE Eng. Med. Biol. Soc.*, Sep. 2009, pp. 2180–2183.
[92] C. P. Warren, S. Hu, M. Stead, B. H. Brinkmann, M. R. Bower, and G. A. Worrell, "Synchrony in normal and focal epileptic brain: The seizure onset zone is functionally disconnected," *J. Neurophysiol.*, vol. 104, no. 6, pp. 3530–3539, Dec. 2010.
[93] A. von Stein and J. Sarnthein, "Different frequencies for different scales of cortical integration: From local gamma to long range alpha/theta synchronization," *Int. J. Psychophysiol.*, vol. 38, no. 3, pp. 301–313, 2000.
[94] O. Jensen and L. L. Colgin, "Cross-frequency coupling between neuronal oscillations," *Trends Cognit. Sci.*, vol. 11, no. 7, pp. 267–269, Jul. 2007.
[95] R. T. Canolty, E. Edwards, S. S. Dalal, M. Soltani, S. S. Nagarajan, H. E. Kirsch, M. S. Berger, N. M. Barbaro, and R. T. Knight, "High gamma power is phase-locked to theta oscillations in human neocortex," *Science*, vol. 313, no. 5793, pp. 1626–1628, Sep. 2006.
[96] R. T. Canolty and R. T. Knight, "The functional role of cross-frequency coupling," *Trends Cognit. Sci.*, vol. 14, no. 11, pp. 506–515, Nov. 2010.
[97] S. A. Weiss, G. P. Banks, G. M. McKhann, R. R. Goodman, R. G. Emerson, A. J. Trevelyan, and C. A. Schevon, "Ictal high frequency oscillations distinguish two types of seizure territories in humans," *Brain*, vol. 136, no. 12, pp. 3796–3808, Dec. 2013.
[98] S. A. Weiss, A. Lemesiou, R. Connors, G. P. Banks, G. M. McKhann, R. R. Goodman, B. Zhao, C. G. Filippi, M. Nowell, R. Rodionov, B. Diehl, A. W. McEvoy, M. C. Walker, A. J. Trevelyan, L. M. Bateman, R. G. Emerson, and C. A. Schevon, "Seizure localization using ictal phase-locked high gamma: A retrospective surgical outcome study," *Neurology*, vol. 84, no. 23, pp. 2320–2328, Jun. 2015.
[99] M. Le Van Quyen, C. Adam, J. Martinerie, M. Baulac, S. Clémenceau, and F. Varela, "Spatio-temporal characterizations of non-linear changes in intracranial activities prior to human temporal lobe seizures," *Eur. J. Neurosci.*, vol. 12, no. 6, pp. 2124–2134, Jun. 2000.
[100] M. X. Cohen, "Assessing transient cross-frequency coupling in EEG data," *J. Neurosci. Methods*, vol. 168, no. 2, pp. 494–499, Mar. 2008.
[101] A. C. E. Onslow, R. Bogacz, and M. W. Jones, "Quantifying phase–amplitude coupling in neuronal network oscillations," *Prog. Biophys. Mol. Biol.*, vol. 105, nos. 1–2, pp. 49–57, Mar. 2011.
[102] A. B. L. Tort, R. Komorowski, H. Eichenbaum, and N. Kopell, "Measuring phase-amplitude coupling between neuronal oscillations of different frequencies," *J. Neurophysiol.*, vol. 104, no. 2, pp. 1195–1210, 2010.
[103] A. B. Tort, M. A. Kramer, C. Thorn, D. J. Gibson, Y. Kubota, A. M. Graybiel, and N. J. Kopell, "Dynamic cross-frequency couplings of local field potential oscillations in rat striatum and hippocampus during performance of a T-maze task," *Proc. Natl. Acad. Sci. USA*, vol. 105, no. 51, pp. 20517–20522, Dec. 2008.
[104] J. M. Hurtado, L. L. Rubchinsky, and K. A. Sigvardt, "Statistical method for detection of phase-locking episodes in neural oscillations," *J. Neurophysiol.*, vol. 91, no. 4, pp. 1883–1898, Apr. 2004.
[105] B. Elahian, M. Yeasin, B. Mudigoudar, J. W. Wheless, and A. Babajani-Feremi, "Identifying seizure onset zone from electrocorticographic recordings: A machine learning approach based on phase locking value," *Seizure*, vol. 51, pp. 35–42, Oct. 2017.
[106] M. Dümpelmann, "Early seizure detection for closed loop direct neurostimulation devices in epilepsy," *J. Neural Eng.*, vol. 16, no. 4, Aug. 2019, Art. no. 041001.
[107] Y. Park, L. Luo, K. K. Parhi, and T. Netoff, "Seizure prediction with spectral power of EEG using cost-sensitive support vector machines," *Epilepsia*, vol. 52, no. 10, pp. 1761–1770, 2011.
[108] Z. Zhang and K. K. Parhi, "Low-complexity seizure prediction from iEEG/sEEG using spectral power and ratios of spectral power," *IEEE Trans. Biomed. Circuits Syst.*, vol. 10, no. 3, pp. 693–706, Jun. 2016.
[109] M. K. Siddiqui, R. Morales-Menendez, X. Huang, and N. Hussain, "A review of epileptic seizure detection using machine learning classifiers," *Brain Informat.*, vol. 7, no. 1, pp. 1–18, Dec. 2020.
[110] U. R. Acharya, Y. Hagiwara, and H. Adeli, "Automated seizure prediction," *Epilepsy Behav.*, vol. 88, pp. 251–261, Nov. 2018.
[111] Y. Varatharajah, B. Berry, J. Cimbalnik, V. Kremen, J. Van Gompel, M. Stead, B. Brinkmann, R. Iyer, and G. Worrell, "Integrating artificial intelligence with real-time intracranial EEG monitoring to automate interictal identification of seizure onset zones in focal epilepsy," *J. Neural Eng.*, vol. 15, no. 4, Aug. 2018, Art. no. 046035.
[112] D. Lai, X. Zhang, K. Ma, Z. Chen, W. Chen, H. Zhang, H. Yuan, and L. Ding, "Automated detection of high frequency oscillations in intracranial EEG using the combination of short-time energy and convolutional neural networks," *IEEE Access*, vol. 7, pp. 82501–82511, 2019.
[113] A. V. Medvedev, G. I. Agoureeva, and A. M. Murro, "A long short-term memory neural network for the detection of epileptiform spikes and high frequency oscillations," *Sci. Rep.*, vol. 9, no. 1, pp. 1–10, Dec. 2019.
[114] J. Craley, E. Johnson, C. C. Jouny, D. Hsu, R. Ahmed, and A. Venkataraman, "SZLoc: A multi-resolution architecture for automated epileptic seizure localization from scalp EEG," in *Proc. Med. Imag. Deep Learn. (MIDL)*, Zürich, Switzerland, Jul. 2022. [Online]. Available: https://openreview.net/forum?id=yGgZ3iPrkJT
[115] D. Wulsin, J. Blanco, R. Mani, and B. Litt, "Semi-supervised anomaly detection for EEG waveforms using deep belief nets," in *Proc. 9th Int. Conf. Mach. Learn. Appl.*, Dec. 2010, pp. 436–441.
[116] X. Jia, K. Li, X. Li, and A. Zhang, "A novel semi-supervised deep learning framework for affective state recognition on EEG signals," in *Proc. IEEE Int. Conf. Bioinf. Bioeng.*, Nov. 2014, pp. 30–37.
[117] J. C. Bulacio, L. Jehi, C. Wong, J. Gonzalez-Martinez, P. Kotagal, D. Nair, I. Najm, and W. Bingaman, "Long-term seizure outcome after resective surgery in patients evaluated with intracranial electrodes," *Epilepsia*, vol. 53, no. 10, pp. 1722–1730, Oct. 2012.
[118] Y. Lu, G. A. Worrell, H. C. Zhang, L. Yang, B. Brinkmann, C. Nelson, and B. He, "Noninvasive imaging of the high frequency brain activity in focal epilepsy patients," *IEEE Trans. Biomed. Eng.*, vol. 61, no. 6, pp. 1660–1667, Jun. 2014.
[119] G. Pellegrino, T. Hedrich, R. Chowdhury, J. A. Hall, J.-M. Lina, F. Dubeau, E. Kobayashi, and C. Grova, "Source localization of the seizure onset zone from ictal EEG/MEG data," *Hum. Brain Mapping*, vol. 37, no. 7, pp. 2528–2546, Jul. 2016.

SAI SANJAY BALAJI (Graduate Student Member, IEEE) received the B.E. degree in electronics and instrumentation engineering from Anna University, Chennai, in 2015, and the M.S. degree in electrical and computer engineering from the University of Minnesota, Minneapolis, MN, USA, in 2021, where he is currently pursuing the Ph.D. degree in electrical engineering.

KESHAB K. PARHI (Fellow, IEEE) received the B.Tech. degree from IIT Kharagpur, Kharagpur, in 1982, the M.S.E.E. degree from the University of Pennsylvania, Philadelphia, in 1984, and the Ph.D. degree from the University of California at Berkeley, Berkeley, in 1988. He has been with the University of Minnesota, Minneapolis, since 1988, where he is currently a Distinguished McKnight University Professor and an Edgar F. Johnson Professor of electronic communication with the Department of Electrical and Computer Engineering. He has published over 680 articles and the inventor of 32 patents. He has authored the textbook *VLSI Digital Signal Processing Systems* (Wiley, 1999). His current research interests include VLSI architecture design of machine learning systems, hardware security, data-driven neuroscience, and molecular/DNA computing. He is a fellow of the ACM, AIMBE, AAAS, and NAI. He was a recipient of numerous awards, including the Mac Van Valkenburg Award, in 2017, the Charles A. Desoer Technical Achievement Award, in 2012, the IEEE Kiyo Tomiyasu Technical Field Award, in 2003, and a Golden Jubilee Medal from the IEEE Circuits and Systems Society, in 2000. He served as the Editor-in-Chief for the IEEE TRANSACTIONS ON CIRCUITS AND SYSTEMS I: REGULAR PAPERS, from 2004 to 2005.